





Environmental memory facilitates search with home returns

Amy Altshuler,^{1,2} Ofek Lauber Bonomo ^{1,2} Nicole Gorohovsky ^{1,3} Shany Marchini,^{1,3} Eran Rosen,¹ Ofir Tal-Friedman,⁴ Shlomi Reuveni ^{1,2,5,*,\dagger} and Yael Roichman ^{1,2,4,*,\ddagger}

¹The Raymond and Beverley School of Chemistry, Tel Aviv University, Tel Aviv 6997801, Israel

²Center for Physics and Chemistry of Living Systems, Tel Aviv University, Tel Aviv 6997801, Israel

³Department of Materials Science and Engineering, Tel Aviv University, Tel Aviv 6997801, Israel

⁴The Raymond and Beverley School of Physics & Astronomy, Tel Aviv University, Tel Aviv 6997801, Israel

⁵Sackler Center for Computational Molecular & Materials Science, Tel Aviv University, Tel Aviv 6997801, Israel



(Received 23 July 2023; accepted 2 May 2024; published 6 June 2024)

Search processes in the natural world are often punctuated by home returns that reset the position of foraging animals, birds, and insects. Many theoretical, numerical, and experimental studies have now demonstrated that this strategy can drastically facilitate search, which could explain its prevalence. To further facilitate search, foragers also work as a group: modifying their surroundings in highly sophisticated ways, e.g., by leaving chemical scent trails that imprint the memory of previous excursions. Here, we design a controlled experiment to show that the benefit coming from such environmental memory is significant even for a single, nonintelligent searcher that is limited to simple physical interactions with its surroundings. To this end, we employ a self-propelled bristle robot that moves randomly within an arena filled with obstacles that the robot can push around. To mimic home returns, we reset the bristle robot's position at constant time intervals. We show that trails created by the robot give rise to a form of environmental memory that facilitates search by increasing the effective diffusion coefficient. Numerical simulations and theoretical estimates designed to capture the essential physics of the experiment support our conclusions and indicate that these are not limited to the particular system studied herein.

DOI: [10.1103/PhysRevResearch.6.023255](https://doi.org/10.1103/PhysRevResearch.6.023255)

I. INTRODUCTION

Search processes are common in nature, from animal foraging on the macroscopic scale [1,2] to the search of biomolecules inside living cells [3,4]. Over the years, search and first-passage problems attracted considerable attention in different fields and contexts [5–7]. It has been widely observed that a proper choice of the stochastic mode of motion can significantly facilitate search. Finding optimal search strategies in different conditions and under various constraints has thus become a central goal of search research [8–14].

Recently, a series of theoretical, computational, and experimental studies demonstrated that resetting a search process repeatedly can accelerate it regardless of the underlying mode of stochastic motion [15–22], and as long as the first-passage time distribution without resetting is sufficiently dispersed [23]. This counterintuitive fact was pointed out as a major advantage of search with home returns [24] that is prevalently displayed by foraging animals, birds, and insects.

Missing completely from the discussion and analysis of resetting, and search with home returns, are interactions between the searching agent and its environment. For example, autochemotactic cells mark and sense their environment [25–27], thus building memory which can in turn be used to expedite search [28]. Similarly, ants (and other insects) mark the ground with chemical scents while foraging and navigating back and forth from the nest in search of a food source [29,30]. Here again, memory is gradually built into the environment, which means that the first search attempt is different from the second, which is in turn different from the third, and so on and so forth.

Ants tend to follow dominant scent trails that were previously used and marked by many ants, indicating that scent trails provide effective means of communication. This environment-mediated interaction between foraging ants helps expedite the process of finding food and carrying it back home [31–34]. Inspired by the amazing ability of a cooperating collective to improve search efficiency by chemically imprinting the memory of past events onto its surroundings; we ask a fundamental question: Can simple physical interactions between a single, nonintelligent searcher and its environment facilitate target location?

Here, we address this question within a controlled experimental setup: A bristle robot searching in a field of movable obstacles. Bristle robots are devices that convert the kinetic energy of vibration into forward propulsion using their flexible bristlelike legs [35]. They exhibit persistent random

*These authors contributed equally to this work.

^{\dagger}shlomire@tauex.tau.ac.il

^{\ddagger}roichman@tauex.tau.ac.il

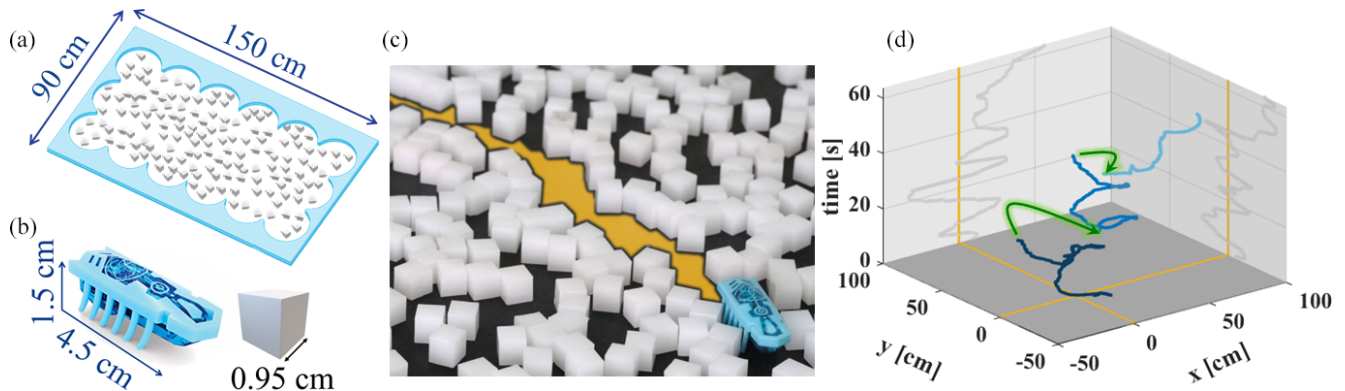


FIG. 1. The experimental setup. (a) A sketch detailing the arena and its dimensions (the inner dimensions are $137 \times 63 \text{ cm}^2$). (b) Characteristic scales of the bbot and the mobile cubic obstacles. (c) An image of a bbot (in blue) paving its way through the arena and leaving a trail (orange). (d) Sample trajectory of the bbot (in shades of blue) and its projections onto the axes (in gray). Resetting events are marked with green arrows.

motion [35,36] and have been applied to study swarm robotics [37,38] and statistical mechanics out of thermal equilibrium [39–41].

In our experiment, collisions with the movable obstacles allow the bristle robot to imprint memory onto its environment and simultaneously “sense”, via excluded volume interactions, the presence of obstacles and of trails it formed previously. The robot is given a fixed time window to explore the arena. At the end of this time interval, to mimic a home return via an existing trail, the robot is returned to its starting position without erasing the trails it created previously. This process is performed repeatedly, resulting in significant reshaping of the arena such that it is partitioned into clear trails and denser obstacle islands. Comparing these experiments to ones in which we scramble the arena to erase the robot’s footprints, we demonstrate the benefits of environmental memory on search with home returns.

A. Encoding memory and sensing using mechanical interactions

Figures 1(a) and 1(b) depict details of the experimental setup. We employ commercially available self-propelled bristle robots (bbots, Hexbug’s Nano Newton series) and analyze their motion in an arena (outer $150 \times 90 \text{ cm}^2$ and inner $137 \times 63 \text{ cm}^2$ dimensions) containing cubic mobile obstacles (0.95^3 cm^3 Perspex cubes, $m = 1 \text{ g}$). Bbots are active particles that convert electric energy stored in a battery to vibrations. The tilted elastic legs of the bbots transform the vibrations to persistent forward motion [with some chirality, Supplemental Material (SM) [42] Fig. 1]. Since active particles tend to move along boundaries, we fashion the arena’s edges in a way that injects the bbots inwards and away from the boundaries. The area fraction of the mobile obstacles in the arena was set to $\phi = 0.3$.

When a bbot is introduced to the arena, it clears obstacles from its path by colliding with them [see Fig. 1(c) and SM video S1], which is typical for active particles in crowded environments [43,44]. At later times, it can either return to previously cleared trails, create new trails, or destroy existing ones. Thus, the trail pattern formed in the arena remembers the bbot’s path, which we will henceforth refer to as environ-

mental memory or simply just memory. Similar environmental memory was observed on microscopic scales in a mixtures of active and passive particles [44]. Since the bbot moves more freely when it revisits previously cleared trails, environmental memory also feeds back onto the bbot’s motion. We record the motion of the bbot using a webcam (BRIO 4K, Logitech) at a rate of 60 FPS. We use conventional particle tracking algorithms [45] to extract trajectories.

We perform resetting experiments using the following protocol: Initially, the obstacles are scattered randomly across the arena. The experiments start by releasing a bbot from the center of the arena. The bbot then carves its path by pushing aside obstacles that it encounters. Following a fixed time interval from its release, or if the bbot reaches the arena boundaries, the bbot is plucked out of the arena and repositioned at the origin. Thus, the bbot’s position is reset (SM video S2). This procedure is aimed to mimic random search followed by the bbot’s return home via an existing trail. The bbot is positioned at a new orientation after each resetting event to ensure uniform sampling of the initial direction of motion. The manual resetting process is cut out of the recorded trajectories of the bbot. An excerpt of a typical trajectory, including two resetting events, is shown in Fig. 1(d).

B. Environmental memory enhances mobility

To study the effect of environmental memory on the steady-state distribution of the bbot and its passage times to a certain location in the arena, i.e., the search time, we perform two sets of experiments: with and without environmental memory. In the experiments with environmental memory, only the bbot’s position is reset while obstacles are untouched. In contrast, in the experiments without environmental memory, we manually rescatter the obstacles upon resetting. Rescattering of the obstacles results in full resetting of the system: the bbot’s position and its environment. We use a resetting protocol in which the bbot is reset approximately at constant time intervals of $\tau = 20 \text{ s}$, i.e., sharp resetting [17,46–48]. In addition, in both experiment versions, we reset the bbot’s position when it reaches the arena’s boundaries. The resulting resetting time distribution (SM Fig. 4) is spread

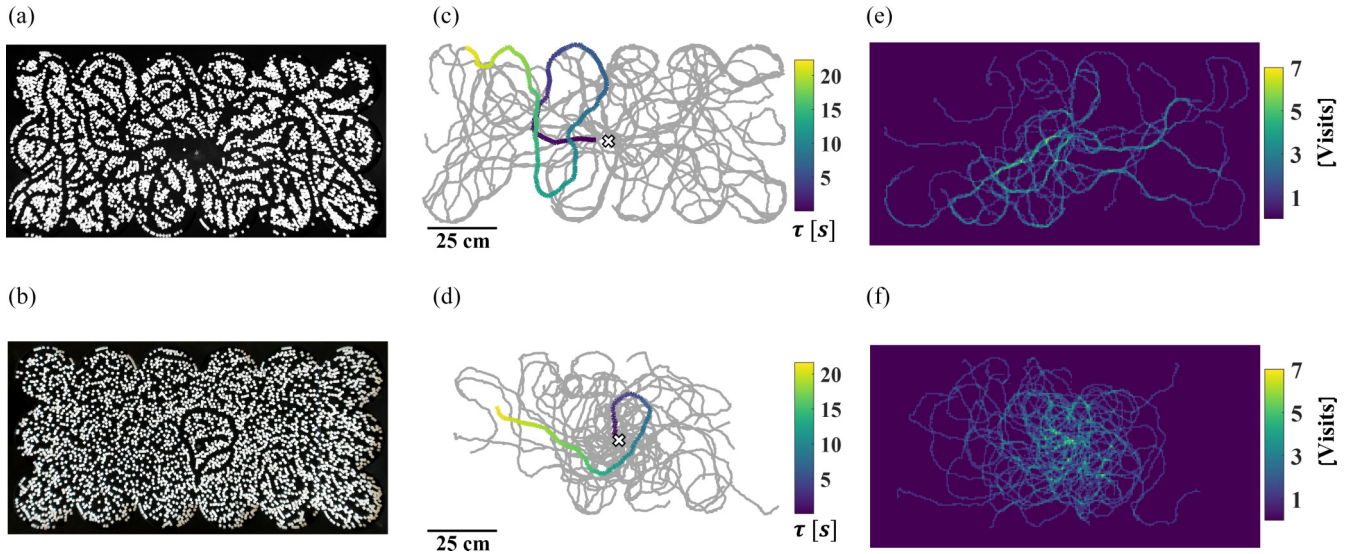


FIG. 2. Comparison of typical arenas and the bbot's motion with and without environmental memory, top and bottom panels, respectively. (a), (b) Images of typical arenas with and without memory, 30 min into the experiment. (c), (d) Trajectories of the bbot with and without memory (in gray). The colored trajectories show the evolution in time of a single trail. A white cross marks the origin. (e), (f) Histograms of the number of visits to different locations in the arena with 0.25^2 cm^2 sized bins.

between $\approx 5 \text{ s}$ to $\approx 25 \text{ s}$ with an average of $\langle R \rangle = 13.2 \pm 5.7 \text{ s}$ and $\langle R \rangle = 12.9 \pm 5.6 \text{ s}$ for experiments with and without memory, respectively. We stress that, regardless of the resetting event type, the sharp resetting timer starts fresh when the bbot's position is reset to the origin.

In Figs. 2(a) and 2(b), we show snapshots of the arena 30 minutes into the start of the experiment. The difference between Fig. 2(a) (with memory) and Fig. 2(b) (without) results in different characteristics of the ensemble of trajectories shown in Figs. 2(c) and 2(d) (gray lines). Near the origin, the trajectories are sparser in the system with memory and denser in the system without. This observation implies that, in experiments with environmental memory, the bbot tends to revisit and stabilize existing trails. As a result, we observe striking differences in trajectory patterns. Specifically, the occurrence of extended trails is enhanced in the presence of environmental memory. We further visualize this effect in Figs. 2(e) and 2(f), where we present histograms of the number of visits to different locations in the arena. Quantifying the persistence length of the bbot from orientation correlation decay of typical trajectories, we find $\ell_p = 14.3 \text{ cm}$ (with memory) and $\ell_p = 10.0 \text{ cm}$ (without), which provides quantitative support to the observations made above.

One of the hallmarks of random motion with resetting is the emergence of a nonequilibrium steady state for the position of the reset particle [20]. Such a steady state is also reached in our experiments when considering the position of a bbot that is reset without keeping environmental memory. However, the situation is more complicated when we allow the environment to retain the memory of the bbot's motion, as the arena itself also evolves with time. In experiments conducted with environmental memory, the bbot constantly creates and destroys previous trails. As a result, obstacles are dynamically rearranged until the bbot's environment reaches a quasi-steady-state (see SM Figs. 2 and 3 for quantitative assessment).

We characterize the bbot's motion and the resulting position distribution under these quasi-steady-state conditions. First, we calculate the typical mean squared displacement (MSD) of the bbot along the long axis of the arena, which we henceforth denote as x . We concentrate our analysis on the x axis, as the robot's motion along the y axis exhibits similar behavior but is more sensitive to edge effects. The MSD is computed by taking an average, over all N resetting events, of the bbot's squared displacement

$$\langle \Delta x^2(t) \rangle = \frac{1}{N} \sum_{i=1}^N (\Delta x_i(t))^2, \quad (1)$$

where $\Delta x^2(t) = (x(t) - x(0))^2$, and t is the lag time since the last resetting event. In Fig. 3(a), the MSD of the bbot is shown for the two sets of experiments, with and without memory. Both curves have a similar shape starting with a short superdiffusive segment that transitions into a diffusive (linear) regime, as expected for persistent motion in the presence of obstacles [49]. Indeed, the bbot performs directed motion at short timescales and is scattered randomly by collisions with the obstacles at longer times. Eventually, the bbot reaches the boundaries and is reset. Therefore, we truncate the MSD curves at a cutoff that is smaller than the typical time it takes the bbot to reach the arena's boundaries. The diffusion coefficient of the bbot's motion is extracted from the slope of the MSD at the linear regime. We find $D = 34.7 \pm 0.3 \text{ cm}^2/\text{s}$ and $D = 21.9 \pm 0.2 \text{ cm}^2/\text{s}$ with and without memory, providing further support for the observation that the bbot diffuses more efficiently with memory, i.e., when it can revisit existing trails. Thus, the faster motion along a previously carved trail allows the robot to reach further before being reset, leading to an enhanced diffusion coefficient in a system with memory.

To further quantify this effect, we measure the probability distribution of the bbot's position along the long axis of the arena at a given time, t , indicating the lag time from the

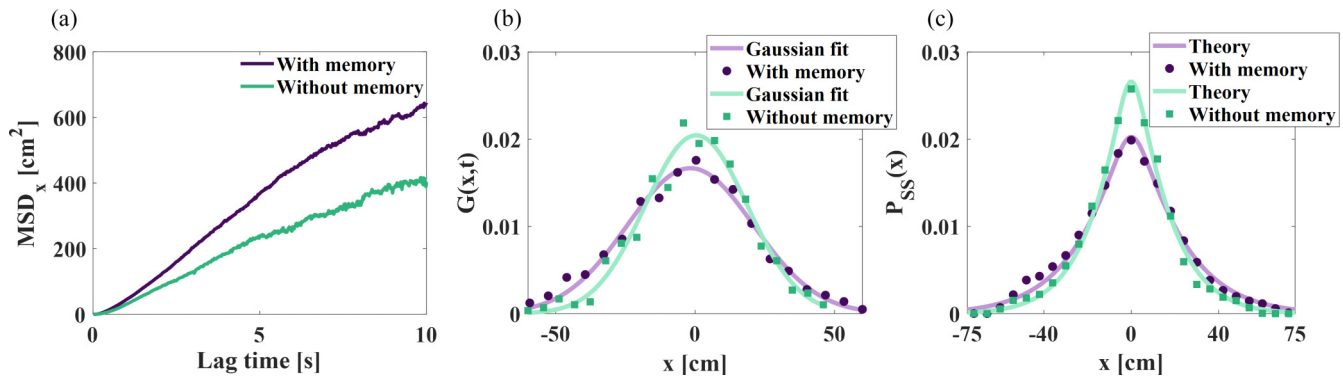


FIG. 3. Characteristics of the bbot’s motion within the quasi-steady-state phase, with and without memory. (a) MSD as a function of the lag time, calculated from an ensemble of $N = 1223$ (with memory) and $N = 670$ (without memory) resetting events. (b) Position distributions along the x axis, at a lag time $t = 5$ s from a resetting event. Experimental measurements (markers) and fits to Eq. (2) (solid lines). (c) Steady-state position distributions of the bbot along the x axis, for resetting with and without memory. Experimental measurements (markers) and fits to Eq. (3) (solid lines). In all panels, observe the enhanced mobility under environmental memory conditions.

previous resetting event [Fig. 3(b)]. In agreement with our previous observation, the distribution of position in a system with memory is wider. In addition, we find that this distribution is roughly Gaussian

$$G(x, t|x_0, 0) = \frac{1}{\sqrt{4\pi Dt}} e^{-\frac{(x-x_0)^2}{4Dt}}, \quad (2)$$

thus allowing us to map the problem to that of a particle performing free diffusion with an effective diffusion coefficient D , where x_0 is the origin.

The steady-state distribution of diffusion under Poissonian, i.e., constant rate, resetting has a cusp at the origin and exponentially decaying tails [15,20]. Here, resetting is conducted at (nonexponential) random time intervals taken from the resetting time distribution in SM Fig. 4. Thus, we observe a smoother steady-state position distribution $P_{ss}(x)$ of the bbot along the x axis [Fig. 3(c)]. Moreover, the functional form of $P_{ss}(x)$ is similar to that of a normally diffusing particle undergoing resetting in an obstacle-free system,

$$P_{ss}(x) = \frac{1}{\langle R \rangle} \int_0^\infty \frac{\Psi(t)}{\sqrt{4\pi Dt}} e^{-\frac{(x-x_0)^2}{4Dt}} dt, \quad (3)$$

where $\Psi(t)$ is the survival function of the resetting time R , i.e., the probability that the resetting time R is larger than a threshold time t (SM Fig. 5), and $\langle R \rangle$ is the mean resetting time. This prediction of $P_{ss}(x)$ fits well the experimental data of both systems, with and without memory. The effective diffusion coefficients extracted from the fits are $D = 42.73$ cm²/s and $D = 24.49$ cm²/s, with and without memory, respectively. The obtained values are similar to the ones extracted from MSD measurements.

C. Environmental memory facilitates search

Having established that memory enhances the bbot’s mobility, we now turn to quantify the effect of memory on search. We introduce a target line to our setup at $x = 40$ cm [see Fig 4(a)]. We look at a sequential series of search processes, each starting at the origin and ending at the target. For each search process, we define the passage time (PT) as the time it takes the bbot to reach the target starting from the origin. Note that the PT includes all the resetting events that happened

prior to the bbot’s arrival at the target. We also reset the bbot’s position after it reaches the target. In experiments without environmental memory, we manually rescatter the obstacles after each resetting event and when the bbot reaches the target.

In some cases, the bbot does not reach the target during the entire 30 min duration of the experiment. Therefore, we first measure the fraction of experiments in which the bbot reached the target. We find that for a system with memory, $N_{\text{reach}}/N_{\text{total}} = 329/330 \sim 99\%$, whereas $N_{\text{reach}}/N_{\text{total}} = 79/82 \sim 96\%$ for a system without memory. This indicates that the probability of reaching the target in systems with memory is slightly higher.

For bbots that were able to reach the target, we also measure the probability density function of the PTs, and plot it for experiments with and without memory in Fig. 4(b). Averaging over these distributions, we find that the normalized mean passage times (MPTs) are given by $\langle \text{PT} \rangle / \tau = 4.7 \pm 0.4$ and $\langle \text{PT} \rangle / \tau = 9.3 \pm 1.2$ for systems with and without memory, respectively. Note, that these numbers report means and

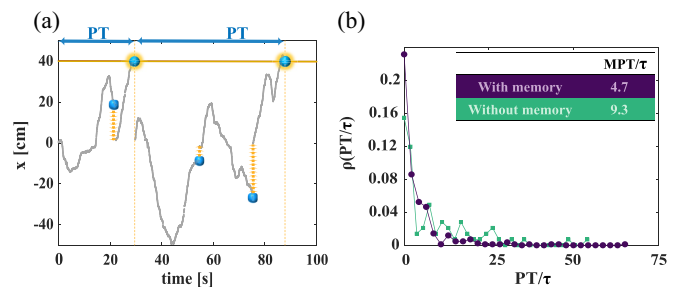


FIG. 4. Characteristics of search under resetting. (a) Projection of the bbot’s trajectory onto the x axis in a typical experiment showing two instances in which the bbot reached the target. The two PTs are marked using double-headed, blue arrows. The target is positioned at $x = 40$ cm and is marked by a yellow line. Resetting events are marked using a series of arrows pointing back at the origin. (b) Comparison between the probability density functions of PTs with and without memory. Here, the PT is taken in units of the time, τ , between sharp resetting events. Markers come from experiments, and continuous lines are used as a guide to the eye. The MPTs with and without memory are indicated in the inset.

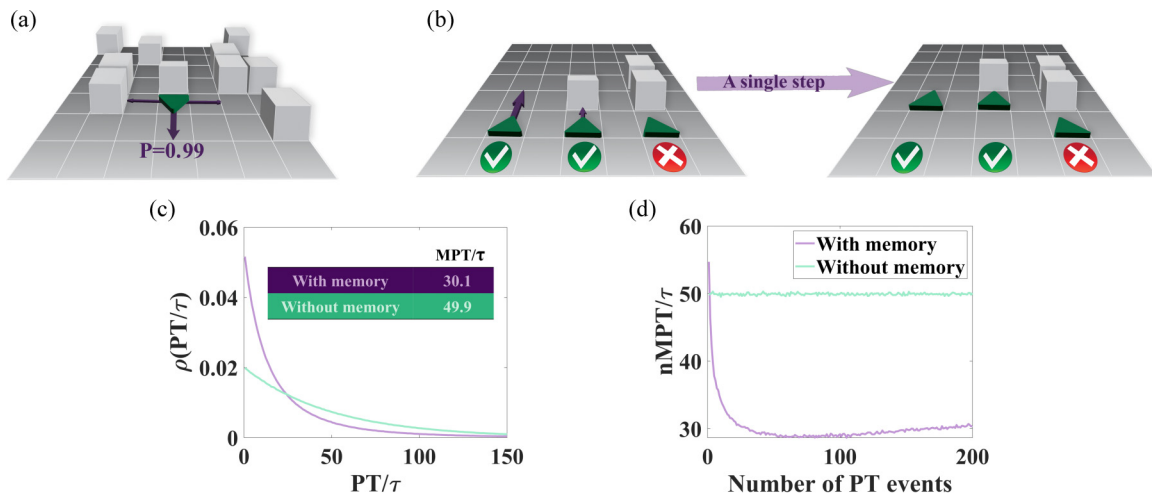


FIG. 5. (a), (b) The persistent *Sokoban* random walk and its laws of motion. (c) Comparison between the probability density functions of PTs with and without memory. Here, the PT is taken in units of the time, τ , between sharp resetting events. The MPTs with and without memory are indicated in the inset. (d) The mean n th passage time (nMPT) as a function of the number of PTs at the beginning of the simulation. In simulations with memory, obstacles are scattered only at the beginning of the simulations. Hence memory is continuously encoded into the environment, and the nMPT first sharply decreases and then slightly increases to the value reported in the inset of (c). In contrast, in simulations without memory obstacles are rescattered after every resetting event. Thus, the nMPT remains constant.

standard errors in the estimation of the means in units of the sharp resetting time τ . We thus find that memory significantly reduces the time it takes a bbot to reach the target line in our experiment.

D. Revealing the buildup of environmental memory

Memory in the environment is built gradually, increasing with every resetting event and the subsequent redistribution of obstacles in the arena. As a result, we also expect the MPT to decrease gradually, as time progresses, from a value close to that of a system without memory to that of a system with memory. The latter is expected when the obstacles' configuration in the arena reaches a steady state. However, capturing this transition requires much more data than is realistically attainable in experiments. Thus, instead, we use Monte Carlo simulations to show that the predicted effect is also seen in a stylized model that captures the essential physics governing our experiment. To this end, we adapt the *Sokoban* random walk, which has recently been introduced to explore the effect of tracer-media interactions on motion and transport in disordered media [50].

In the *Sokoban* simulations, a random walker of unit size moves on a rectangular, 151×91 , arena with mobile obstacles of unit size scattered throughout [Fig. 5(a)]. The area fraction of the mobile obstacles in the arena was set to $\phi = 0.3$, as in the experiments. At each time step, the random walker tries to move one step in a random direction relative to the direction of its last step. To imitate a bbot's motion, we make the walker persistent by taking the probability of forward motion to be 0.99, and the probability turning and moving either left or right to be 0.005. Additional rules were implemented to take into account interactions between the random walker and the obstacles scattered across the arena [Fig. 5(b)], namely, a move always takes place if the walker tries to move into an unoccupied site. Otherwise, the walker

may try to move into an occupied site by pushing an obstacle one site forward (in the direction of motion). However, such a move will only take place if the site to which the obstacle is pushed is vacant. In other words, unlike in experiments, the *Sokoban* walker cannot push multiple obstacles simultaneously (SM video S3). If a forbidden step is attempted, the walker stays put at that given time step.

Next, we performed simulations using a resetting protocol that is almost identical to that used in the experiments. Obstacles are scattered randomly across the arena, and the simulation starts by releasing the walker at its center. The walker then carves its path by pushing aside obstacles that it encounters. As in the experiments, we implement sharp resetting by returning the walker to the origin at constant time intervals of $\tau = 2000$ time steps, or when it reached the boundaries of the arena. The resulting resetting time distributions are shown in SM Fig. 7, along with the survival functions. We stress that, regardless of the resetting event type, the sharp resetting timer starts fresh when the walker's position is reset to the origin. To ensure uniform sampling of the initial direction of motion, the walker is positioned at a new orientation after each resetting event.

We performed two sets of simulations: with and without environmental memory. In simulations conducted with environmental memory, the arena is left untouched, i.e., it is not randomized after resetting the walker's position. As a result, obstacles are dynamically rearranged until the environment reaches a steady state (SM Fig. 6(a)). In contrast to the experiment, where only a quasi-steady-state is achieved, in the *Sokoban* simulations, a steady state is characterized by obstacle configurations that the walker can no longer modify. Hence, we eventually observe obstacle configurations that are fixed in time. Sample trajectories for simulations with and without memory are shown in SM Figs. 6(b) and 6(c).

To characterize the effect of memory on the walker's motion, we repeated the analysis reported in Fig. 3 for the

simulated data. At short times ($t \leq 50$ steps), we observe the effect of directed motion on the MSD, per expectations and experimental observations. At longer times, the MSD becomes linear with a diffusion constant of $D = 0.119 \pm 0.014$ and $D = 0.073 \pm 0.002$ with and without memory, respectively [SM Fig. 8(a)]. Note that the forward motion probability of the walker was chosen such that the ratio of MSDs, with and without memory will be similar to the experimentally measured one. As in the experiment, we find that the probability distribution of the walker's position along the long axis of the arena is approximately Gaussian. The enhanced mobility of the walker under environmental memory conditions is clearly reflected on the propagator level [SM Fig. 8(b)] and when comparing steady-state position distributions along the x axis [SM Fig. 8(c)].

Having established that memory enhances the walker's mobility, similar to its observed effect in experiments, we turned to quantify the effect of memory on search. We introduced a target line to our simulations at $x = 40$ and collected statistics for the PT to the target. In Fig. 5(c), we compare the probability density functions of the PTs for simulations conducted with and without memory. Following the experiments, simulations with memory were conducted at steady-state conditions of the arena. Similar to the experiments, here too we find that a small fraction of walkers fail to reach the target. These are excluded from the PT distributions. Averaging over the PT distributions, we find that MPTs are given by $\langle \text{PT}/\tau \rangle = 30.1$ and $\langle \text{PT}/\tau \rangle = 49.9$, for systems with and without memory respectively.

Finally, we characterize the change in the MPT due to the structural evolution of the environment as memory is built into the arena. We do so by calculating the mean n th passage time (nMPT), which is averaged over many realizations as a function of the number of PTs since the start of the experiment. In simulations without memory, obstacles are rescattered in the arena after each resetting event. We thus expect the nMPT to remain constant, i.e., not to depend on the passage number and the time elapsed since the onset of the simulation. In contrast, for simulations with memory, we expect the nMPT to decrease with time, evolving with the changes in the obstacles' distribution in the arena from a value close to that of a system without memory to that of a system with memory at steady-state conditions. These expectations are in good agreement with simulation results that are plotted in Fig. 5(d). The transition observed in the simulations agrees with the two limiting conditions measured in experiments.

Concluding this section, we see that the broader implications of our experimental findings become evident through their manifestation in a different model system: the *Sokoban* random walk. While this stylized model differs from our experiment in the fine details of its microscopic dynamics, it nevertheless captures the fundamental physics and is able to qualitatively reproduce main results. Intriguingly, we find that motion in the model must be persistent to reproduce the decrease in search time resulting from environmental memory. This finding emphasizes that environmental memory from the type studied here must be paired with persistent motion in order to benefit search.

E. Long-term memory leads to ergodicity breaking

Since the bbot effectively displays diffusive behavior, it is only natural to ask if the measured values of the diffusion coefficients can be used to provide a theoretical estimate that captures the experimental MPTs. To answer this question, we construct a simplified model of our experiments. We assume that (i) the bbot's motion can be described by simple diffusion, (ii) motion along the x direction is independent of motion along the y direction, and (iii) resetting occurs after a fixed time τ or when one of the boundaries at the y direction is reached. This neglects resetting events from the far boundary ($x = -68.5$ cm), which are relatively rare. For resetting without memory, these simplifications allow us to approximate the MPT using a known formula from the theory of first-passage under restart.

Letting T denote the passage time without resetting and R denote a statistically independent resetting time, we have $\langle \text{PT} \rangle = \frac{\langle \min(T, R) \rangle}{\text{Pr}(T < R)}$ [17]. To apply this formula in our case, we approximate T with the analytically known first-passage time of diffusion in an interval with an absorbing boundary at $x = 40$ cm and a reflecting boundary at $x = -68.5$ cm. To approximate R , we take the minimum between the sharp resetting time τ and the analytically known first-passage time of diffusion in an interval with absorbing boundaries at $y = +31.5$ cm and $y = -31.5$ cm. The mean of the minimum of T and R can then be easily calculated, and the same goes for the probability that first passage will occur before resetting. Overall, taking $D = 21.9$ cm²/s that was extracted from the experiment and $\tau = 20$ s, this calculation gives $\langle \text{PT}/\tau \rangle \approx 6.04$. Performing a similar calculation for the *Sokoban* random walk without memory (note the slightly different arena dimensions), we plug in $D = 0.073$ and $\tau = 2000$, and find $\langle \text{PT}/\tau \rangle \approx 52$.

While these theoretical estimates show good agreement with the *Sokoban* MPT reported in Fig. 5(c), there is a relative error of approximately $\approx 35\%$ compared to the experimental MPT reported in Fig. 4(b). One potential source of error is the nondiffusive nature of the bbot's motion at timescales shorter than the persistence time. To address this issue, we also conducted simulations of our simplified diffusion model, keeping the target line and resetting rules consistent with the experiment. For short time steps, $dt \ll \ell_p^2/2D$, we obtained an MPT that matched the theoretical prediction as expected. Increasing the simulation time step to $dt = \ell_p^2/2D \approx 2.28$ s, and repeating the simulations we got $\langle \text{PT}/\tau \rangle \approx 8.16$, which agrees with experiments (to measurement error). Consequently, we conclude that the lion's share of the error associated with the theoretical prediction originates from the nondiffusive behavior of the bbot at short timescales.

Finally, we ask whether results obtained in the presence of environmental memory can also be understood in a similar fashion. At face value, the answer to this question should be no. The formula used above is based on the renewal assumption, which implies that the past is forgotten after a resetting event and thus passage attempts are statistically independent and identical. Clearly, this assumption does not hold for experiments with environmental memory. Surprisingly, when performing the same calculation as before to estimate the MPT theoretically with $D = 34.7$ cm²/s (the measured diffusion coefficient with memory), we obtain $\langle \text{PT}/\tau \rangle \approx 3.54$.

This value yields a relative error of approximately $\approx 25\%$, which is comparable to the error observed in the absence of memory. Furthermore, similar to the no-memory case, this error almost vanishes when accounting for the nondiffusive behavior of the bbot at short timescales as before.

We thus conclude that the memory in our experiment primarily influences the effective diffusion coefficient of the bbot; and that once this is known, correlations between passage attempts are not strong enough to create significant deviations from the renewal-based theoretical prediction. This can be understood by noting that the bbot scrambles the arena during its motion, which renders correlations short-ranged in time.

The situation is drastically different for the *Sokoban* in the presence of environmental memory. Unlike the experiment, *Sokoban* arenas evolve until they reach a fixed configuration of obstacles that the random walker can no longer alter. This means that the renewal assumption, following resetting events, is asymptotically exact in the long time limit of a single trajectory. However, for $D = 0.119$ obtained from *Sokoban* simulations with memory, the theoretical estimate yields $(PT/\tau) \approx 14.95$, which is half the true value. We attribute this discrepancy to the breakdown of ergodicity. The reported diffusion coefficient is based on an ensemble average over numerous arena configurations. In contrast, for each time trace, a single configuration becomes fixed. i.e., there is no averaging in time. To show that this is indeed the primary source of error, we modified the *Sokoban* simulation such that a new *steady-state configuration* of the arena is sampled with each resetting event. We then recover good agreement with the theoretical estimate, reducing the relative error to approximately $\approx 15\%$.

Concluding this section, we see that one significant difference between simulations of the *Sokoban* random walk and our experiments is the timescale over which environmental memory persists. In the *Sokoban* model, the distribution of obstacles across the arena reaches a steady-state configuration that is frozen in time. Thus, the system does not self-average over time, and ergodicity is broken. This ergodicity breaking is different from the inherent ergodicity breaking of resetting processes [51]. In contrast, in the experiment, obstacles constantly move: trails are formed and destroyed such that a dynamic quasi-steady-state is reached. Crucially, the bristle robot continues to scramble the arena in its motion, which renders memory and correlation times finite. We expect this to change in experiments with higher obstacle densities (SM Fig. 9), which give rise to longer-lasting memory and non-ergodic behavior. Clearly, another theoretical framework to understand resetting in the presence of memory and strong temporal correlations will then be required. A more detailed characterization of the effect of obstacle density on search and mobility is left for future work.

II. CONCLUSION

By itself, the ability to mark and sense the environment does not improve or detract from the efficiency of a search process. Yet organisms such as ants and bacteria found ways to expedite the search for nutrients by use of chemical markings that relay information to the future self (and other

searchers) via the environment. It is natural to ask, What is the level of complexity required of a searcher to implement such mechanisms to better its search? Can a simple physical mechanism facilitate search by encoding environmental memory?

We conducted a controlled experiment to measure the impact of environmental memory on motion and target location. We showed that even a single, nonintelligent searcher—a bristle robot—can expedite its search by taking advantage of mechanical interactions that combine the ability to mark and perceive the environment. Using a resetting protocol, we demonstrated that environmental memory—manifested as obstacle-free trails—significantly improved the robot’s mobility; consequently leading to a broader distribution of the bristle robot’s location and reduced search times.

Our results suggest that any memory encoding (and sensing) method, such as mechanical, chemical, or optical, which enhances the speed or spread of the searching agent, will lead to lower search times. Moreover, since memory encoded in the environment can also be used by other searchers, our study extends to search involving multiple searchers originating from the same place, although we neglect direct interactions between the searchers. Enhanced mobility will also expedite the detection of targets with varying sizes and dimensions.

Here, we focused on elucidating the primary effects of environmental memory on search, leveraging the theoretical framework of resetting to quantify its ramifications. While we focused on a relatively simple setting, broad conclusions coming from our study are expected to apply more generally. For example, our choice of the return method—instantaneous returns—can be extended to finite-time returns, such as direct returns at constant velocity. It is a reasonable assumption that the searcher knows its way home and does not need to search for it. The arising question is whether ballistic returns negate the effect of memory on search. To assess this, we notice that the enhanced mobility of a searcher in a system with memory has two opposing effects on the temporal overhead of returns compared to a system without memory. On the one hand, it increases the distance that the searcher should return from, thus increasing the mean return time. On the other hand, it reduces the number of search trials, thus reducing the mean number of returns per first passage event. This competition between diffusive spreading and ballistic returns can be analyzed quantitatively (see SM discussion on the effect of ballistic returns on the search time). Clearly, for high return velocities—the limit of instantaneous returns—search benefits from environmental memory as illustrated above. Moreover, for the systems analyzed here, we find this remains the case regardless of the return velocity.

Enhanced mobility improves search by allowing the searcher to reach further away in less time. Yet, in systems with environmental memory, this may come at the expense of area coverage. Note, however, that in the conditions of our experiment, this should not prevent the detection of localized targets since environmental memory is short-ranged. It is thus virtually impossible that the access to certain regions, or targets, will be blocked by obstacles. In contrast, in systems exhibiting kinetically locked nonergodic environments, such as in the *Sokoban* model, there can be situations where certain regions of the arena are inaccessible, thus detracting from search efficiency. The competition between enhanced

mobility and area coverage is currently under investigation, specifically in systems with larger obstacle densities.

Our findings also bring to the forefront a theoretical challenge. The current theoretical framework aimed to predict first passage under resetting is based on the renewal assumption. This assumption is clearly violated where environmental memory is long-ranged, which leads to significant prediction errors. A suitable theoretical framework is thus required to better understand resetting in the presence of memory and strong temporal correlations.

In conclusion, we studied the effect of environmental memory on search with home returns and showcased its benefits in well-controlled laboratory experiments and numerical simulations. It is now essential to explore how complexity influences environment-assisted search strategies by taking a fundamental physics perspective. For instance, how do nonlinear effects arising from environmental reorganization impact search efficiency? And what is the effect of different strengths, types, and durations of trail markings? Introducing

agent complexity, such as memory, sensing, communication, and computational capabilities—which are common in swarm robotics—is expected to further amplify search performance. Yet, a quantitative understanding of the added value brought by these elements is clearly missing. Progress in this direction may also shed light on how living organisms use environmental memory to facilitate search.

ACKNOWLEDGMENTS

S.R. acknowledges support from the Israel Science Foundation (Grant No. 394/19). This project has received funding from the European Research Council (ERC) under the European Union's Horizon 2020 research and innovation program (Grant Agreement No. 947731). Y.R. acknowledges support from the Israel Science Foundation (Grants No. 988/17 and No. 385/21) and from the European Research Council (ERC) under the European Union's Horizon 2020 research and innovation program (Grant Agreement No. 101002392).

-
- [1] G. M. Viswanathan, M. G. E. da Luz, E. P. Raposo and H. E. Stanley, *The Physics of Foraging: An Introduction to Random Searches and Biological Encounters* (Cambridge University Press, 2011).
- [2] E. Kagan and I. Ben-Gal, *Search and foraging: Individual motion and swarm dynamics* (CRC Press, Boca Raton, Florida, 2015).
- [3] P. H. von Hippel and O. G. Berg, Facilitated target location in biological systems, *J. Biol. Chem.* **264**, 675 (1989).
- [4] P. Hammar, P. Leroy, A. Mahmutovic, E. G. Marklund, O. G. Berg and J. Elf, The lac repressor displays facilitated diffusion in living cells, *Science* **336**, 1595 (2012).
- [5] S. Redner, *A Guide to First-Passage Processes* (Cambridge University Press, New York, USA, 2001).
- [6] R. Metzler, G. Oshanin, and S. Redner, *First-Passage Phenomena and Their Applications* (World Scientific, Singapore, 2014).
- [7] A. J. Bray, S. N. Majumdar and G. Schehr, Persistence and first-passage properties in nonequilibrium systems, *Adv. Phys.* **62**, 225 (2013).
- [8] G. M. Viswanathan, S. V. Buldyrev, S. Havlin, M. Da Luz, E. Raposo and H. E. Stanley, Optimizing the success of random searches, *Nature (London)* **401**, 911 (1999).
- [9] M. F. Shlesinger, Search research, *Nature (London)* **443**, 281 (2006).
- [10] I. Eliazar, T. Koren and J. Klafter, Searching circular DNA strands, *J. Phys.: Condens. Matter* **19**, 065140 (2007).
- [11] M. A. Lomholt, K. Tal, R. Metzler and K. Joseph, Lévy strategies in intermittent search processes are advantageous, *Proc. Natl. Acad. Sci.* **105**, 11055 (2008).
- [12] O. Bénichou, C. Loverdo, M. Moreau and R. Voituriez, Intermittent search strategies, *Rev. Mod. Phys.* **83**, 81 (2011).
- [13] G. Volpe and G. Volpe, The topography of the environment alters the optimal search strategy for active particles, *Proc. Natl. Acad. Sci. USA* **114**, 11350 (2017).
- [14] D. Bernardi and B. Lindner, Run with the Brownian hare, hunt with the deterministic hounds, *Phys. Rev. Lett.* **128**, 040601 (2022).
- [15] M. R. Evans and S. N. Majumdar, Diffusion with stochastic resetting, *Phys. Rev. Lett.* **106**, 160601 (2011).
- [16] L. Kusmierz, S. N. Majumdar, S. Sabhapandit and G. Schehr, First order transition for the optimal search time of Lévy flights with resetting, *Phys. Rev. Lett.* **113**, 220602 (2014).
- [17] A. Pal and S. Reuveni, First passage under restart, *Phys. Rev. Lett.* **118**, 030603 (2017).
- [18] A. Chechkin and I. M. Sokolov, Random search with resetting: A unified renewal approach, *Phys. Rev. Lett.* **121**, 050601 (2018).
- [19] O. Tal-Friedman, A. Pal, A. Sekhon, S. Reuveni and Y. Roichman, Experimental realization of diffusion with stochastic resetting, *J. Phys. Chem. Lett.* **11**, 7350 (2020).
- [20] M. R. Evans, S. N. Majumdar and G. Schehr, Stochastic resetting and applications, *J. Phys. A: Math. Theor.* **53**, 193001 (2020).
- [21] O. Blumer, S. Reuveni and B. Hirshberg, Stochastic resetting for enhanced sampling, *J. Phys. Chem. Lett.* **13**, 11230 (2022).
- [22] R. Yin and E. Barkai, Restart expedites quantum walk hitting times, *Phys. Rev. Lett.* **130**, 050802 (2023).
- [23] A. Pal, S. Kostinski and S. Reuveni, The inspection paradox in stochastic resetting, *J. Phys. A: Math. Theor.* **55**, 021001 (2022).
- [24] A. Pal, Ł. Kuśmierz and S. Reuveni, Search with home returns provides advantage under high uncertainty, *Phys. Rev. Res.* **2**, 043174 (2020).
- [25] E. Ben-Jacob, I. Cohen and H. Levine, Cooperative self-organization of microorganisms, *Adv. Phys.* **49**, 395 (2000).
- [26] W. T. Kranz, A. Gelimison, K. Zhao, G. C. Wong and R. Golestanian, Effective dynamics of microorganisms that interact with their own trail, *Phys. Rev. Lett.* **117**, 038101 (2016).
- [27] J. Taktikos, V. Zaburdaev and H. Stark, Modeling a self-propelled autochemotactic walker, *Phys. Rev. E* **84**, 041924 (2011).

- [28] H. Meyer and H. Rieger, Optimal non-Markovian search strategies with n -step memory, *Phys. Rev. Lett.* **127**, 070601 (2021).
- [29] B. Hölldobler and E. Wilson, *The Ants* (Belknap Press of Harvard University Press, Cambridge, MA, 1990).
- [30] E. David Morgan, Trail pheromones of ants, *Physiol. Entomol.* **34**, 1 (2009).
- [31] D. J. Sumpter and M. Beekman, From nonlinearity to optimality: pheromone trail foraging by ants, *Anim. Behav.* **66**, 273 (2003).
- [32] D. E. Jackson, S. J. Martin, M. Holcombe and F. L. W. Ratnieks, Longevity and detection of persistent foraging trails in Pharaoh's ants, *Monomorium pharaonis* (L.), *A. Anim. Behav.* **71**, 351 (2006).
- [33] I. D. Couzin, Collective cognition in animal groups, *Trends Cognit. Sci.* **13**, 36 (2009).
- [34] E. Fonio, Y. Heyman, L. Boczkowski, A. Gelblum, A. Kosowski, A. Korman, and O. Feinerman, A locally-blazed ant trail achieves efficient collective navigation despite limited information, *eLife* **5**, e20185 (2016).
- [35] L. Giomi, N. Hawley-Weld and L. Mahadevan, Swarming, swirling and stasis in sequestered bots-bots, *Proc. R. Soc. A.* **469**, 20120637 (2013).
- [36] O. Dauchot and V. Démery, Dynamics of a self-propelled particle in a harmonic trap, *Phys. Rev. Lett.* **122**, 068002 (2019).
- [37] A. Deblais, T. Barois, T. Guerin, P. H. Delville, R. Vaudaine, J. S. Lintuvuori, J. F. Boudet, J. C. Baret, and H. Kellay, Boundaries control collective dynamics of inertial self-propelled robots, *Phys. Rev. Lett.* **120**, 188002 (2018).
- [38] J. F. Boudet, J. Lintuvuori, C. Lacouture, T. Barois, A. Deblais, K. Xie, S. Cassagnere, B. Tregon, D. B. Brückner, J. C. Baret, and H. Kellay, From collections of independent, mindless robots to flexible, mobile, and directional superstructures, *Sci. Rob.* **6**, eabd0272 (2021).
- [39] P. Baconnier, D. Shohat, C. H. López, C. Coulais, V. Démery, G. Düring and O. Dauchot, Selective and collective actuation in active solids, *Nat. Phys.* **18**, 1234 (2022).
- [40] M. Dasgupta, S. Guha, L. Armbruster, D. Das, and M. K. Mitra, Non-monotonic behavior of timescales of passage in heterogeneous media: Dependence on the nature of barriers, [arXiv:2211.13814](https://arxiv.org/abs/2211.13814).
- [41] K. Engbring, D. Boriskovsky, Y. Roichman and B. Lindner, A nonlinear fluctuation-dissipation test for Markovian systems, *Phys. Rev. X* **13**, 021034 (2023).
- [42] See Supplemental Material at <http://link.aps.org/supplemental/10.1103/PhysRevResearch.6.023255> for supplementary Figs. 1–9, supplementary discussion on the effect of ballistic returns on the search time, and supplementary movies 1–3.
- [43] A. Biswas, J. M. Cruz, P. Parmananda and D. Das, First passage of an active particle in the presence of passive crowders, *Soft Matter* **16**, 6138 (2020).
- [44] C. S. Dias, M. Trivedi, G. Volpe, N. A. M. Araújo, and G. Volpe, Environmental memory boosts group formation of clueless individuals, *Nature Commun.*, **14**, 7324 (2023).
- [45] J. C. Crocker and D. G. Grier, Methods of digital video microscopy for colloidal studies, *J. Colloid Interface Sci.* **179**, 298 (1996).
- [46] A. Pal, A. Kundu and M. R. Evans, Diffusion under time-dependent resetting, *J. Phys. A: Math. Theor.* **49**, 225001 (2016).
- [47] U. Bhat, C. D. Bacco and S. Redner, Stochastic search with Poisson and deterministic resetting, *J. Stat. Mech.: Theory Exp.* (2016) 083401.
- [48] I. Eliazar and S. Reuveni, Mean-performance of sharp restart I: Statistical roadmap, *J. Phys. A: Math. Theor.* **53**, 405004 (2020).
- [49] C. Bechinger, R. Di Leonardo, H. Löwen, C. Reichhardt, G. Volpe, and G. Volpe, Active particles in complex and crowded environments, *Rev. Modern Phys.* **88**, 045006 (2016).
- [50] O. L. Bonomo and S. Reuveni, Loss of percolation transition in the presence of simple tracer-media interactions, *Phys. Rev. Res.* **5**, L042015 (2023).
- [51] R. Goerlich, M. Li, L. B. Pires, P.-A. Hervieux, G. Manfredi, and C. Genet, Experimental test of Landauer's principle for stochastic resetting, [arXiv:2306.09503](https://arxiv.org/abs/2306.09503).